Acoustic Emission Monitoring and Thrust Network Analysis of the Central Nave Vaults of the Turin Cathedral

Acoustic Emission Monitoring and Thrust Network Analysis of the Central Nave Vaults of the Turin Cathedral

Amedeo Manuello[1][0000−0003−1474−0176], Francesco Marmo[2][0000−0002−3456−2867], Jonathan Melchiorre[1][0000−0002−8721−8365]

[1] Department of Structural, Geotechnical and Building Engineering, Politecnico di Torino, Corso Duca degli Abruzzi, 24 - 10129. Torino, Italy,
amedeo.manuellobertetto@polito.it

[2] Department of Structures for Engineering and Architecture, Università degli Studi di Napoli Federico II - Corso Umberto I 40 - 80138 Napoli

Abstract. Due to their age, elevation, and prolonged exposure to both static and dynamic loading conditions, historical constructions and old masonry structures such as medieval and Gothic cathedrals, bell towers, and other similar structures, are particularly vulnerable. The central nave vault of the Turin cathedral was subjected to an acoustic emission (AE) monitoring technique for structural integrity assessment. These findings are correlated with the evidence from the Thrust Network Analysis (TNA) performed on the cathedral's central nave vault, taking into account the additional elements added at the start of the XXth century to lessen horizontal forces. In this situation, the analysis's findings are strictly correlated to the vault's 3D AE localization, which was obtained by the triangulation method.

Keywords: Acoustic Emission · b-value analysis · AE source localization · Thrust Network Analysis · Masonry vaults

1 Introduction

Due to numerous coexisting circumstances operating on the bearing materials (thermal loading, static and dynamic loading, subsidence, fatigue, and creep), historical buildings commonly exhibit ubiquitous fracture patterns. We can evaluate the preservation status of these structures and their temporal evolution using non-destructive techniques [1–6]. In the past few years, numerous research have been carried out in historic masonry buildings using a control mechanism based on the spontaneous emission of elastic waves [7–9]. Through AE monitoring, wide-band piezoelectric (PZT) sensors capture the signals produced by microcracks (100–350 kHz), which are then post-processed by statistical and analytical analysis [10]. The authors gained extensive expertise in the monitoring of ancient structures using the AE technique, including masonry towers and monuments with stone bearing walls, as well as conventional and sack masonry systems [7, 9]. The Syracuse cathedral's vertical bearing structure was monitored

using the AE approach to manage the progression of structural damage brought on by pre-seismic and seismic activity. The Asinelli's Tower in Bologna, Central Italy, is an example of how the AE signals were employed simultaneously to evaluate the impact of recurring phenomena (motor traffic loads, wind effects) [8, 9]. The results of AE monitoring for an array of eight pzt sensors installed on the central nave vault of the Turin cathedral were first analyzed in the current study. The examination of the AE cumulative number and several characteristics that can forecast how the damage behavior will change over time (such as the b-value and β^t). In particular, the b-value analysis reveals a declining trend toward values consistent with the expansion of localized micro and macro-cracks in the monitored structure's component around various locations identified in the vault's 3D model. These results are related to the numerical outcomes of the Thrust Network Analysis (TNA) performed on the vault, taking into account additional elements added at the beginning of the XX century to reduce the horizontal forces, along with supporting evidence from other AE parameters. The TNA is typically used to represent stresses in masonry vaults as a discrete network of forces in equilibrium with gravity loads, based on Heyman's ideas through a graphical interpretation. The 3D localisation is primarily connected with the outcomes of the study based on TNA. In 1694, the naves and the dome were finished. Carlo Filiberto of Savoy hosted the Holy Shroud at the end of the sixteenth century. In this regard, it has been made possible by the historical-critical analysis of the Cathedral of Turin to emphasize that the current structure is the result of a number of interventions that create a heterogeneous condition in terms of the materials used as well as the consolidating methods that were used. The first structural intervention was required in 1656 on the occasion of the partial collapse of the central nave's vault. The use of the aforementioned iron chains on the tangential side and the lower surface of the shutters allowed the vault to be stabilized until the successive interventions of the 20th century, which significantly altered the structure of the church attic and led to its current configuration. The vault was judged to be structurally unsafe in 1928. The lunette-adorned barrel-lowered vault was supported by steel beams that were positioned orthogonally to the vault's axis and hooked by iron tie-rods. In particular, there are 13 pairs of double T-shaped beams running the length of the vault extension. These beams are fixed in huge reinforced concrete blocks, 13 on each side, and are positioned in line with the pillars.

2 AE Monitoring analysis and methods

Eight piezoelectric (PZT) transducers are arranged in an array connected to a multi-channel system (each channel having a dedicated memory of 64 Mb), which automatically stores and processes important waveform parameters of the detected signal (the cumulative number of events, signal durations, peak amplitudes, and ring down counts), allowing in situ damage localization and quantification from the recorded parameters. The AE signal frequency connected to the damage evolution is between 200 and 50 times the sampling rate of the

AE device (10 Ms/s) [11]. The threshold methods used in the various cases were implemented in the software of the device used and reported by the authors in several publications [9, 11]. The AE equipment automatically performs different kinds of analyses. The first parameter is represented by the cumulative number of AE signals N, detected during the monitoring time. In addition, the time dependence of the structural damage observed during the monitoring period, identified by parameter β^t, can also be correlated to the rate of the micro-cracks propagation in the time domain. [6–10,24–26]. In the first localization step all the signals, recorded by different sensors, falling into a time intervals compatible with the formation of micro-cracks are recognized ad grouped. In the preliminary studies devoted to AE localization in concrete and concrete structures [12], it was usual to assume that the amplitude threshold of 100 mV of the non-amplified AE signal was appropriate to recognize the onset time of the AE P-wave. The AE localization problem in its traditional form can be written as:

$$d_i - d_j = v_p \Delta t_{ij} \tag{1}$$

where Δt_{ij} is the measured arrival time difference representing the difference of the signal arrival time at the positions of the sensor i and j. At the same time, the velocity v_p may be assumed as a material constant, or according to the damage evolution in the material, as a changing parameters correlated to the damage level. According to this last considerations the estimating variables of the AE localization procedure are the AE source coordinates (x, y, z) and the p-wave elastic propagation velocity. Different groups, composed by at least 5 sensors, must be recognized for each micro-crack to be localized. As far the velocity v_p is concerned the expression is obtained as,

$$v_p = \sqrt{E(1-\nu)/(\rho(1+\nu)(1-\nu))} \tag{2}$$

and for concrete and masonry material assuming $\nu = 0.2$:

$$E = 0.9(v_p^2 \rho) \tag{3}$$

These last assumption allowed to estimated the variation of E according to the evolving damage [13]. The instrumentation noise, the p-wave picking method utilized to assess the signal onset time, etc. can all be related to the accuracy of the AE localization. Regarding the last point, various techniques were employed to determine the best arrival time at each sensor. This suggests that the enhanced AIC picker approach can be applied. Here, the AE code used for the localization of the sources directly implements the improved AIC method, which is based on the Akaike information criterion. The signal is regarded as an AR model using this approach:

$$x_t = \sum_{k=1}^{N} a_m^i x_{j-m} + e_t^i \tag{4}$$

with t = 1, ..., k for interval 1 and t = k + 1, ..., n for interval 2. The model takes into account both the deterministic and non-deterministic components of

the time series. The time series with no fixed order e_t^n or noise, is assumed to be Gaussian. The maximum likelihood estimation (MLE) of the AIC method is used to extract the non-deterministic part of the time series in intervals [1, k] and [k + 1, n] using Eq. (4), where k is the division point. We can express the approximate likelihood function L for the two non-deterministic time series in intervals [1, k] and [k + 1, n] as:

$$L(x; k, M, \Theta) = \prod_{i=1}^{2} \frac{1}{\sigma_i^2 2\pi} exp \frac{1}{\sigma_i^2} \sum_{k=1}^{N} ((a_m^i x_{j-m} + e_t^i)^2) \tag{5}$$

where $\Theta_i(\Theta(a_1^i ..., a_M^i)$ represents the model parameters (σ_i^2 is dependent on k), and $p_1 = 1, p_2 = k + 1, n_1 = k, n_2 = n - k$. By the maximization of the logarithmic form of the function L. Considering the the AIC Criterion as: AIC=-ln(L)+2k and it can be rewritten considering the two portion of the signal the one characterized by the white noise and the second containing the signal:

$$AIC(k) = klog(\sigma_{1,max}^2) + (n - k)log(\sigma_{2,max}) + 2C \tag{6}$$

In this last relation the first term indicates the badness of the model fit and the second the unreliability. Point k where the joint likelihood is maximized, or AIC(k) in Eq. (6) is minimized, determines the optimal separation of the two time series:

$$AIC(k_w) = k_w log(var(R_w(1, k_w))) + (n_w - k_w)log(var(R_w(1 + k_w, n_w))), \tag{7}$$

where the subscript w denotes that not the whole time series is taken, but only the chosen window containing the onset time. n_w, is the last sample of the current time series, kw ranges from 1 to n_w. The term $var(R_w(1, k_w))$ is the variance function calculated from 1 to kw, while $var(R_w(1 + k_w, n_w))$ means that all samples ranging from $1 + k_w$ to n_w are considered. The global minimum of the AIC function defines the first P-wave onset time of the AE signal.

$$\sum_{t=k+1}^{10} |x_t|/10 \geq 4 \sum_{t=1}^{k} |x_t|/k \tag{8}$$

The fourfold mean amplitude of the interval of the time series ranging from 1 to k is compared with the mean amplitude of a shifting set of 10 data using this relation. The predetermined onset time (k_0) is chosen as the first value of k, which satisfies Eq. (8). Always localized after the actual onset time, the first estimation. In the AIC application, two different types of time frames with various time intervals are successively set taking into mind this fact. First, we apply the algorithm to the interval $[1, k_0]$ (window 1), which is used for a rough determination of the onset time by the AIC and gives k1 value. The second time window (2) is considered centered on the value k_1 with a length of $2\Delta k$. The value of Δk depends on the sample frequency. In our study, the sample frequency is 10 MHz, and Δk equal to 3000 samples gives us an ideal result. As the actual onset time of the AE signal under analysis, the time window (2) value $k_m in$ from

the AIC-picker is taken into consideration. The outcomes of the AE localization process based on the modified AIC-picker approach [11] are reported in Figure 1.

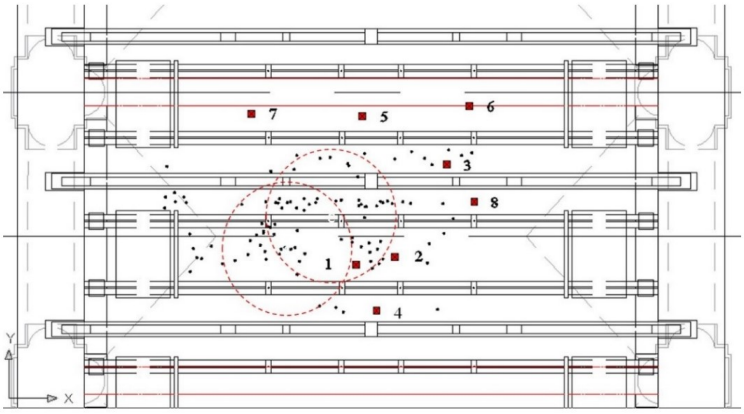

Fig. 1: Plan view of where EA sources are located.

3 Equilibrium analysis of the central nave vault

The stresses that cause a masonry arch or vault collapse are usually lower than those required for the material failure. Therefore, as Heyman pointed out in 1995, the stability of such structures depends mainly on their shape and self-weight distribution [14]. O'Dwyer contributed to its development in 1999 [15], but it was fully developed only in recent years by Block and coworkers (Thrust network analysis) [16, 17]. Other approaches to modeling stresses in masonry vaults can be found in [18–20].

Marmo and Rosati [21] reformulated Block's version of the TNA by avoiding graphical interpretation of the method in order to avoid the employment of the so-called dual grid and focusing solely on the primal grid, resulting in a significant improvement in computational performance. This new version of the TNA incorporates horizontal forces in the analysis, as well as the inclusion of holes or free edges in the vault. Such approach has been successfully applied to a series of case studies including helical staircases [22] and fictile vaults [23]. In this paper it is be employed to analyse the central nave vaults of the Turin Cathedral.

3.1 Limit conditions for the of Turin Cathedral central nave vaults

For the equilibrium analysis of a masonry vault, internal forces can be modelled as a network of thrusts. These thrusts are compression forces that act within

the structure, in equilibrium with the applied loads. This network is henceforth referred to as the *thrust network* in which thrust values associated to branches and the vertical coordinate of nodes are unknown.

Thrust values are required to be compressive, while nodal heights are required to be contained within the masonry thickness. Hence, equilibrium of the network is iused to evaluate unknown branch thrusts and nodal heinghts by employing coupled optimization procedures, fully described in [21], here omitted for brevity.

In general, two extreme solutions are found by the solving procedure, respectively representing the deepest and shallowest configurations of a thrust network, which are characterized by different values of a numeric parameter r, representing a scaling factor of forces applied to the network model. Let r_d (r_s) represent the value of r associated to the deepest (shallowest) configuration of the network. The ratio r_s/r_d reflects the difference between the two extremes of the equilibrated configurations. Since $r_d > r_s$, this ratio is always less than one. Lower r_s/r_d values mean that the deepest and shallowest configurations of the network are very distinct, suggesting a broad range of possible equilibrated solutions for the structure. Such values usually correspond to safer structures. When the r_s/r_d ratio equals one, the deepest and shallowest configurations of the network become indistinguishable, indicating a limit condition of the structure. At this point, only one equilibrated thrust network that fits within the geometric limits exists, and the structure's ultimate strength is reached.

The ratio $r_s/r_d = 1$ is utilized to determine an extreme geometry or a limit loading condition for the structure. This concept has practical applications, such as assessing the geometric safety factor of the vault [14], which involves determining the minimum thickness required for an equilibrated solution. The same approach can be used to determine the limit multiplier for a specific loading scenario. For instance, if the vault experiences a combination of vertical and horizontal forces, the maximum admissible multiplier of horizontal force can be determined by gradually increasing it until the ratio r_s/r_d equals 1.

3.2 Results of the analysis

The geometry of the entire vault, particularly the intrados and extrados, was determined using the geometric survey of the central nave vault. This geometry is used to establish the node horizontal coordinates. The heights of the vault intrados and extrados are utilized as limit heights in the thrust network model. The initial configuration of the thrust network is a grid located on the mid-surface of the vault with a uniform horizontal spacing of $0.44, m \times 0.44, m$. Additional diagonal branches are included to simulate thrusts along the groins of each lunette.

Figure 2 presents a three-dimensional visualization of the thrust network's initial configuration, with the vault's intrados and extrados shaded in gray.

Nodes are loaded by the vault self weight, which is computed assuming a weight per unit volume of $18\,kN/m^3$, and by a load of $5\,kN/m^2$, uniformly distributed on the entire vault extrados. The additional weight of the fillings above the vault spingers and of the concrete blocks placed above the vault springers

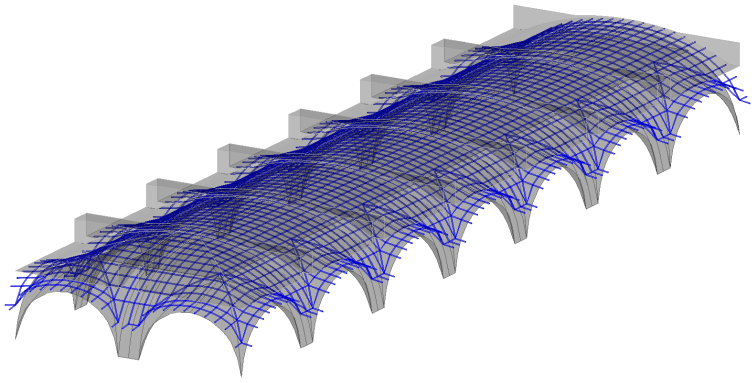

Fig. 2: Initial configuration of the thrust network employed for the equilibrium analysis of the central nave vault.

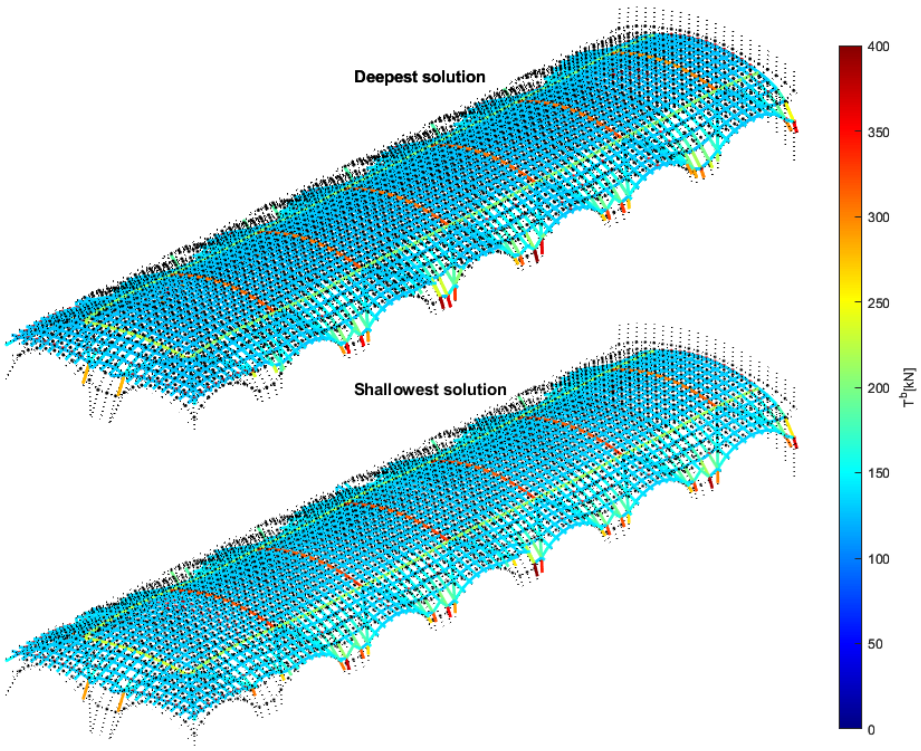

Fig. 3: Deepest and shallowest solutions for the vault having minimum thickness ($T_{min}/T = 0.63$, $R_s/R_d = 1$) subjected to vertical loads only.

during a restoration work carried out at the beginning of the 20th century, each estimated to weight about $61.5\,kN$, was also considered. Following the approach described in [21], the TNA has been applied to evaluate the minimum thickness of the vault, for which the network configurations shown in Figure 3 are obtained.

In addition to the analyses regarding the vault subjected to vertical loads only, we also considered the case of the vault subjected to the combined effect of both vertical and horizontal forces. Horizontal forces were assigned as proportional to the vertical ones and their direction was varied in order to investigate the effect of different orientation of the horizontal loading condition. Accordingly, the horizontal components of nodal forces are assigned as $f_x = |f_z| \cos(\alpha)$, $f_y = |f_z| \sin(\alpha)$, where α is the angle formed by the horizontal action with respect to the x axis of the global reference frame.

Employing the vault symmetry about the longitudinal axis of the nave (i.e. the y axis) the number of significant loading cases is reduced by assuming a total of nine different directions for the horizontal loads, with angular increments of $\pi/8$, spanning between $-\pi/2$, corresponding to forces parallel to the nave and directed towards the narthex, and $\pi/2$, corresponding to forces directed towards the transept. The maximum horizontal load multiplier was computed for each direction of horizontal loads; such solutions are omitted here form brevity.

4 Conclusion

This article presents the monitoring and analysis of the central nave of the Turin Cathedral. The monitoring was conducted using the technique of acoustic emissions, with the installation of 8 different piezoelectric sensors on the structure. The installed instrumentation allowed for the recording of acoustic emission waves caused by the occurrence of fractures within the structure. The improved AIC picker method was then used to identify the onset time of the recorded signals and, consequently, to locate the sources of fractures within the structural elements.

Furthermore, the structure was modeled using the thrust network analysis method to identify the load paths within the vaults. Finally, the method was employed to evaluate the minimum thickness of the vault.

In conclusion, this study demonstrates the application of acoustic emission monitoring for assessing the structural health of the central nave of the Turin Cathedral. The use of piezoelectric sensors and the improved AIC picker method allowed for the detection and localization of fractures within the structure. The thrust network analysis method provided insights into the load paths within the vaults and facilitated the evaluation of the minimum thickness of the vault. These findings contribute to our understanding of the structural behavior and preservation needs of historic masonry structures.

References

1. D. Aggelis, A. Mpalaskas, T. Matikas, Investigation of different fracture modes in cement-based materials by acoustic emission, Cem. Concr. Res. 48 (3) (2013) 1–8.
2. D. Simpson, P. Richards, A probabilistic synthesis of precursory phenomena. in earthquake prediction, / / (2013) 566–574.
3. P. Bak, K. Christensen, L. Danon, T. Scanlon, Unified scaling law for earthquakes, Phys. Rev. Lett. 88 (2002) 178501–1–178501–4.
4. M. Ohtsu, T. Okamoto, S. Yuyama, Moment tensor analysis of acoustic emission for cracking mechanisms in concrete, ACI Struct. J 95 (/) (1998) 87–95.
5. M. M. Rosso, A. Aloisio, J. Melchiorre, F. Huo, G. C. Marano, Noise effects analysis on subspace-based damage detection with neural networks 54 (2023) 23–37.
6. G. Marasco, M. M. Rosso, S. Aiello, A. Aloisio, G. Cirrincione, B. Chiaia, G. C. Marano, Ground penetrating radar fourier pre-processing for deep learning tunnel defects' automated classification, in: Engineering Applications of Neural Networks: 23rd International Conference, EAAAI/EANN 2022, Chersonissos, Crete, Greece, June 17–20, 2022, Proceedings, Springer, 2022, pp. 165–176.
7. A. Anzani, L. Binda, A. Carpinteri, G. Lacidogna, A. Manuello, Evaluation of the repair on multiple leaf stone masonry by acoustic emission 41 (2007) 1169–1189.
8. A. Carpinteri, G. Lacidogna, A. Manuello, G. Niccolini, A study on the structural stability of the asinelli tower in bologna, Struct. Control Health Monit. 23 (/) (2015) 659–667.
9. G. Lacidogna, A. Manuello, A. Carpinteri, Acoustic emission monitoring of italian historical buildings and the case study of the athena temple in syracuse, Architectural Science Review 58 (4) (2015) 290–299.
10. J. Melchiorre, A. Manuello Bertetto, M. M. Rosso, G. C. Marano, Acoustic emission and artificial intelligence procedure for crack source localization, Sensors 23 (2) (2023) 693.
11. A. Carpinteri, J. Xu, G. Lacidogna, A. Manuello, Reliable onset time determination and source location of acoustic emissions in concrete structures, Vol. 34, 2012.
12. S. P. Shah, Z. Li, Localizatin of microcracks in concrete under uniaxial tenssion, ACI Material Journal 91 (4) (1991) 372–381.
13. E. Lenticchia, A. Manuello, C. R., Ae propagation velocity calculation for stiffness estimation in pier luigi nervi's concrete structures, Curved and Layered Structures 8 (1) (2021) 109–118.
14. J. Heyman, The stone skeleton: Structural engineering of masonry architecture, Cambridge University Press (1995).
15. D. O'Dwyer, Funicular analysis of masonry vaults, Computers and Structures 73 (/) (1999) 187–197.
16. P. Block, Thrust network analysis, PhD thesis, Massachusetts Institute of Technology (2009).
17. P. Block, L. Lachauer, Three-dimensional equilibrium analysis of gothic masonry vaults., International Journal of Architectural Heritage 8 (/) (2014) 1–24.
18. M. Angelillo, L. Cardamone, A. Fortunato, A numerical model for masonry - like structures., Journal of Mechanics of Materials and Structures 5 (/) (2010) 415–583.
19. S. Adriaenssens, P. Block, D. Veenendaal, C. Williams, A thrust network approach for the equilibrium problem of unreinforced masonry vaults via polyhedral stress functions., Mechanics Research Communications 37 (/) (2010) 198–204.
20. A. Tralli, C. Alessandri, G. Milani, Computational methods for masonry vaults: a review of recent results, The Open Civil Engineering Journal 8 (/) (2014) 272–287.

21. F. Marmo, L. Rosati, Reformulation and extension of the thrust network analysis., Computers and Structures 182 (/) (2017) 104–118.
22. F. Marmo, D. Masi, L. Rosati, Thrust network analysis of masonry helical staircases, International Journal of Architectural Heritage 12 (5) (2018) 828–848.
23. F. Marmo, N. Ruggieri, F. Toraldo, L. Rosati, Historical study and static assessment of an innovative vaulting technique of the 19th century, International Journal of Architectural Heritage 13 (6) (2019) 799–819.